Direct Evidence for Effects of Grain Structure on Reversible Compressive Deposition Stresses in Polycrystalline Gold Films

J. Leib,* R. Mönig,† and C. V. Thompson

Department of Materials Science and Engineering, Massachusetts Institute of Technology, Cambridge, Massachusetts 02139, USA
(Received 21 February 2009; published 24 June 2009)

A component of the compressive stress that develops during deposition of polycrystalline thin films reversibly changes during interruptions of growth. The mechanism responsible for this phenomenon has been the subject of much recent speculation and experimental work. In this Letter, we have varied the in-plane grain size of columnar polycrystalline gold films with a fixed thickness, by varying their thermal history. Without a vacuum break, the stress in these films was then measured *in situ* during growth and during interruptions in growth. Homoepitaxial gold films were similarly characterized as part of this study. The inverse of the in-plane grain size and the corresponding reversible stress change were found to be proportional, with zero reversible stress change observed for infinite grain size (homoepitaxial films). These results demonstrate a clear role of grain size in the reversible changes in gold films.

Introduction.—There are several stages of stress evolution that occur during deposition of polycrystalline films. Polycrystalline films grow through the Volmer-Weber mechanism in which isolated single-crystal islands nucleate on the surface of the substrate and then grow to coalesce and form a continuous film. Many studies of stress evolution during this process have been carried out [1–3]. When films are grown under conditions of high atomic mobility, the general behavior is as indicated in Fig. 1. As islands coalesce, a tensile stress develops, reaching a peak stress as the films become fully continuous. During continued growth the tensile stress reduces and the stress state usually becomes compressive. There is general agreement in the literature that the initial tensile stress develops due to elastic strain associated with grain boundary formation during island coalescence [4–7]. However, a clear consensus has not emerged with respect to the mechanism that leads to the development of the compressive stress [8–12]. An important additional phenomenon observed during growth of continuous films is that the stress state reversibly changes in the tensile direction during interruptions of growth [3,8–12]. It seems likely that the origin of these reversible stress changes is linked in some way with the mechanism that leads to development of an overall compressive stress state in thicker films. There has been significant speculation in the literature on the origin of these reversible stress changes. Chason *et al.* [10] argued that the compressive stress develops due to adatom trapping at grain boundaries, with the reversible component being associated with outdiffusion from the boundaries near the surface. Spaepen [9] suggested that the reversible changes are the result of outdiffusion of atoms trapped between impinging ledges on growth surfaces. Friesen and Thompson [11] suggested that the reversible changes are associated with differences in surface defect densities on growth and equilibrium surfaces, though recent molecular

dynamics simulations indicate that the stresses associated with surface defects are not high enough to support this argument [13]. Koch, Dongzhi Hu, and Das have also argued that the reversible stress is associated with a surface restructuring that occurs during growth interruptions [12]. Grain boundaries are not included in all of the models, and such effects are still under discussion. A critical assessment of the role of grain boundaries seems to be important and may help to advance our understanding of film growth. The aim of this Letter is to investigate the effect of grain boundaries on stress relaxation.
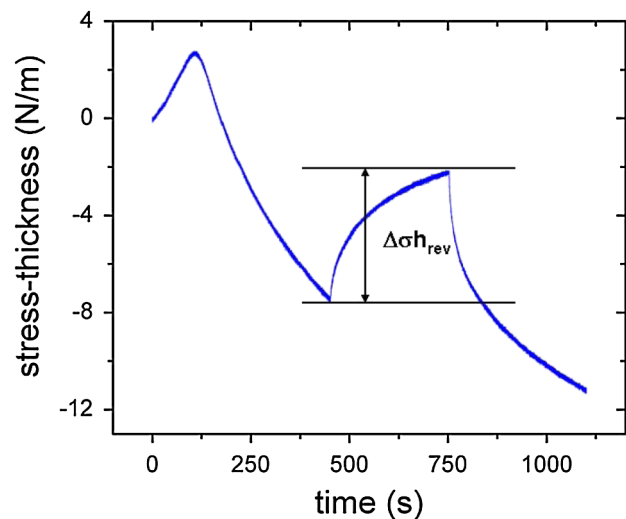

FIG. 1 (color online). Stress-thickness curve for gold deposited at 0.1 nm/s on stress-free silicon nitride. The growth was interrupted after 450 s and resumed after 750 s. The reversibility of stress for continuous films is illustrated, with the change in magnitude at 300 s defined as $\Delta \sigma h_{rev}$ and the change in stress over the same time period as $\Delta \sigma_{rev}$.

Silicon nitride substrate

Deposit 50 nm Au   Deposit 25 nm Au   Deposit 25 nm Au

Rest at RT, 16 h   8 h anneal at 200C,
16 h total

Deposit 25 nm Au   Deposit 25 nm Au
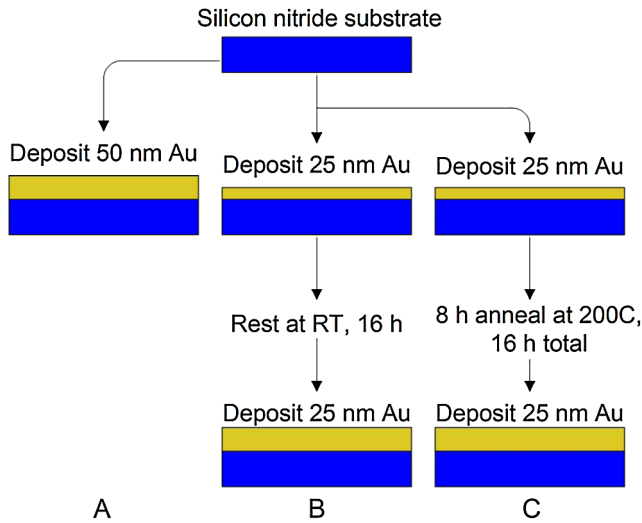
A   B   C

FIG. 2 (color online).   Process flow for generating samples with different mean grain sizes.

Experiments and results.—The polycrystalline films used in this study were $99.99 + \%$ pure gold grown on silicon-nitride-coated (100) silicon wafers. The low-stress 33-nm-thick silicon nitride layers were grown using chemical vapor deposition. Gold deposition was carried out in an ultrahigh vacuum (UHV) electron beam evaporation system with a base pressure of 2×10^{-10} Torr. A quartz crystal monitor (calibrated using atomic force microscopy) was used to monitor deposition rates. Substrates were cleaved into rectangular cantilevers and supported at one end. Deflection of the end of the cantilever during deposition was monitored *in situ* 3.4 cm from the cantilever support using the capacitance measured between a stationary 5 mm^2 circular plate and the curving substrate. Tip deflections as small as 1 nm could be measured at a rate of 100 Hz and were converted to stress using Stoney's equation [14].

To determine the effect of grain structure when other variables were held constant, the following experiments were conducted. First, control samples (samples of type *A*) were created by continuously depositing gold at 0.1 nm/s on low-stress silicon-nitride-coated silicon cantilever sub-

strates at room temperature (23 °C). The tensile stress rise was recorded for 300 s after the deposition was interrupted when the films reached a thickness of 50 nm. The second set of samples (samples of type *B*) was generated by depositing 25-nm-thick gold layers at 0.1 nm/s on unused cantilevers at room-temperature. The samples were allowed to rest at room-temperature for 16 hours before deposition was resumed at 0.1 nm/s. At a total thickness of 50 nm, the deposition was interrupted and the stress recorded. The final set of samples (type *C*) was generated by depositing 25-nm-thick gold layers at 0.1 nm/s on unused cantilevers at room temperature. The samples were kept on the sample stage inside the UHV chamber where they were annealed at 200 °C for 8 hours. After cooling back to room temperature, they were held for another 8 hours before deposition was resumed at 0.1 nm/s. At a total thickness of 50 nm the deposition was interrupted and the stress recorded. The process flow for each set of samples is illustrated in Fig. 2. These three processes led to films with grains through the thickness of the film. Despite having the same thickness, the three films had distinctly different mean grain sizes.

Membranes for transmission electron microscopy (TEM) were created from each (100) cantilever by wet-etching the silicon from the back side of the cantilever with a solution of 25% hydrofluoric acid, 35% nitric acid, and water, after scribing a mask hole into the silicon nitride coating on the back of the cantilever. The silicon nitride on the front side of the cantilever, on which the gold was deposited, acted as an etch stop so that a composite membrane of 33-nm-thick silicon nitride and 50-nm-thick gold spanned the hole in the Si cantilever, which served as a "frame" for the membrane. This process allowed generation of TEM foils within about 30 minutes after stress measurements were completed. For TEM inspection, an accelerating voltage of 200 kV was used. Representative micrographs from the three types of polycrystalline films are shown in Fig. 3. The mean in-plane grain size was determined using the linear intercept method for several film locations and images (not shown), and the average distance between intercepts [15] was 33 nm, 56 nm, and 94 nm for samples *A*, *B*, and *C*, respectively (see Table I). It
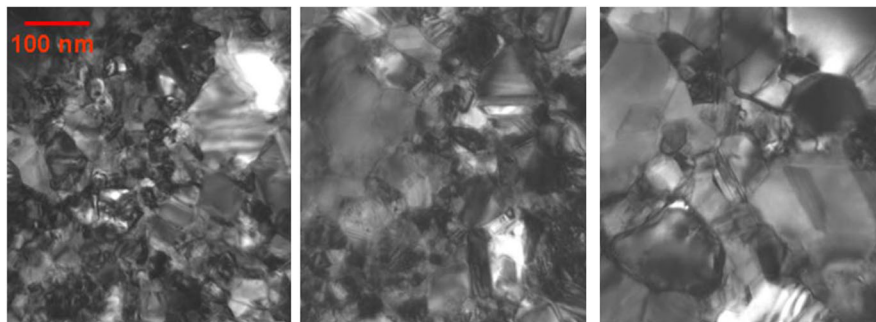
FIG. 3 (color online).   Representative plan view TEM micrographs of, from left to right, sample types *A*, *B*, and *C*.

TABLE I.   Median grain size and the corresponding stress relaxation that occurs during a growth interruption after 300 s of film growth.

Sample	A	B	C	Epitaxial
Median in-plane grain size	33 nm	56 nm	94 nm	Infinite
Tensile stress relaxation after 300 s	80 MPa	46 MPa	29 MPa	<1 MPa

is generally known that grain structures resulting from deposition of polycrystalline films are columnar even when the in-plane grain size is smaller than the film thickness [16]. We therefore expect that most of the grain boundaries in these gold films traverse the thickness of the film.

It should be noted that the difference in the in-plane mean grain size for samples A and B indicates that grain growth occurred during the room-temperature "anneal" of sample B. Evidence of grain growth can also be seen in sample A, and is consistent with early reports of room-temperature grain growth in Au films [17].

An epitaxial gold film was also studied for comparison with the polycrystalline films. In this case, 250 nm of gold was deposited directly on H-terminated (111) silicon cantilevers that had been etched using a 2% HF solution to remove the native oxide before film deposition. This film was then relaxed for 24 hours to be used as the substrate for continued homoepitaxial deposition. As before, 50 nm of gold was deposited at a rate of 0.1 nm/s, and stress evolution was characterized when the deposition was terminated. After deposition, x-ray pole figure analysis confirmed that the gold film had a (111) out-of-plane orientation. It consisted of domains with two in-plane domain orientations, $[1\bar{1}0]$Au ∥ $[1\bar{1}0]$Si and $[\bar{1}10]$Au ∥ $[\bar{1}10]$Si, corresponding to either fcc-like or hcp-like stacking relative to the substrate.

The reversible stress $\Delta\sigma_{rev}$ was defined as of the stress change measured 300 s after interruption of growth of a film of thickness h, as shown in Fig. 1. Figure 4 shows measured values of $\Delta\sigma_{rev}$ for all four of the sample types described above. In contrast with results previously reported for comparable epitaxial Cu and Ag films [11], no detectable reversible stress change was observed for the epitaxial gold films. Recent investigations of homoepitaxial Cu and Ag films carried out using a different sensor and thermal calibration procedure indicated that, as for gold, there was no reversible stress change during growth interruptions for these materials as well. Polycrystalline samples of type A (with the least annealing) had the largest stress rise, and samples of type C (with the most annealing) showed the smallest.

Figure 5 shows the magnitude of the tensile stress rise 300 s after growth termination versus the inverse of the mean grain size (which is proportional to the grain boundary length per unit film area). The trend shown in Fig. 5 is linear within experimental error, and the polycrystalline data extrapolate to a y intercept of zero, consistent with the data for epitaxial films.

Conclusions.—The tensile stress relaxation that occurs during interruptions of growth of polycrystalline gold films scales directly with the grain boundary length per unit area of film surface, and no reversible stress evolution is observed during interruptions of growth of homoepitaxial films. These observations are consistent with the model
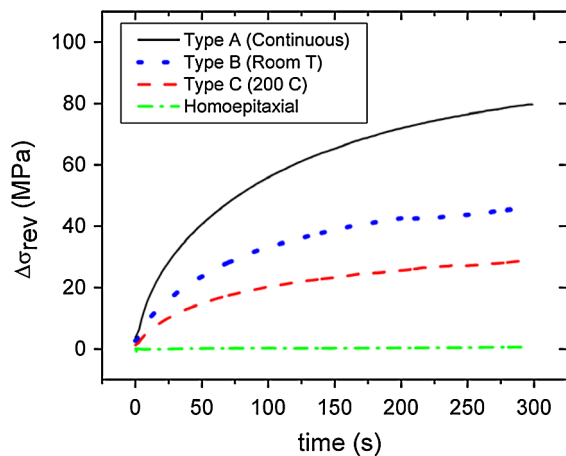

FIG. 4 (color online).   Tensile stress increase after interrupting deposition for the three types of polycrystalline samples and for the homoepitaxial sample.
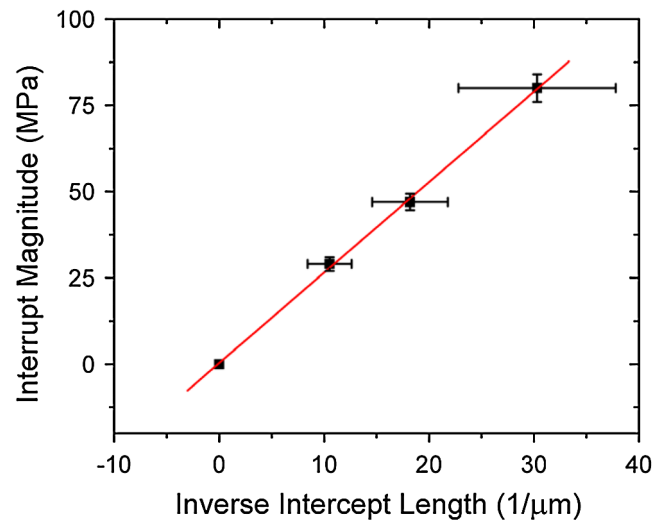

FIG. 5 (color online).   Change in stress for sample types A, B, and C after 300 s plotted against inverse intercept length. The homoepitaxial stress measurement is plotted at an infinite grain size for comparison.

proposed for the mechanism of reversible stress relaxation proposed by Chason *et al.* [10]. However, it is important to note that the correlation established in this Letter does not include a kinetic characterization of the reversible process, nor does it separate the contributions of reversible processes and irreversible processes associated with stress relaxation or microstructural evolution [12]. Further studies are required to fully characterize the reversible relaxation phenomenon.

*Present address: 5200 NE Elam Young Parkway, m/s RA3-301, Intel Corp., Hillsboro, OR 97124, USA.
jeffrey.s.leib@intel.com

†Present address: Institut für Materialforschung II, Forschungszentrum Karlsruhe, Postfach 3640, 76021 Karlsruhe, Germany.
reiner.moenig@imf.fzk.de

[1] R. Abermann and R. Koch, Thin Solid Films **129,** 71 (1985).

[2] J. A. Floro, S. J. Hearne, J. A. Hunter, P. Kotula, E. Chason, S. C. Seel, and C. V. Thompson, J. Appl. Phys. **89,** 4886 (2001).

[3] A. L. Shull and F. Spaepen, J. Appl. Phys. **80,** 6243 (1996).

[4] R. W. Hoffman, Thin Solid Films **34,** 185 (1976).

[5] W. D. Nix and B. M. Clemens, J. Mater. Res. **14,** 3467 (1999).

[6] S. C. Seel, C. V. Thompson, S. J. Hearne, and J. A. Floro, J. Appl. Phys. **88,** 7079 (2000).

[7] L. B. Freund and E. Chason, J. Appl. Phys. **89,** 4866 (2001).

[8] R. C. Cammarata, T. M. Trimble, and D. J. Srolovitz, J. Mater. Res. **15,** 2468 (1999).

[9] F. Spaepen, Acta Mater. **48,** 31 (2000).

[10] E. Chason, B. W. Sheldon, L. B. Freund, J. A. Floro, and S. J. Hearne, Phys. Rev. Lett. **88,** 156103 (2002).

[11] C. Friesen and C. V. Thompson, Phys. Rev. Lett. **93,** 056104 (2004).

[12] R. Koch, Dongzhi Hu, and A. K. Das, Phys. Rev. Lett. **94,** 146101 (2005).

[13] C.-W. Pao, D. J. Srolovitz, and C. V. Thompson, Phys. Rev. B **74,** 155437 (2006).

[14] G. G. Stoney, Proc. R. Soc. A **82,** 172 (1909).

[15] ASTM Designation E 112-60T.

[16] C. V. Thompson, Annu. Rev. Mater. Sci. **30,** 159 (2000).

[17] C. C. Wong, H. I. Smith, and C. V. Thompson, Appl. Phys. Lett. **48,** 335 (1986).